Int. J. Electrochem. Sci., 10 **(2015)** 6405 - 6421

International Journal of
ELECTROCHEMICAL
SCIENCE
www.electrochemsci.org

Charge–transfer Complexation and Photostability Characteristics of Iodine with bis-1,8-naphthalimide as a Photosensitive Biologically Active Units in Solution and in the Solid State: Linear Correlation of Photostability and Dissociation Energy

Moamen S. Refat[1,2,*], *Abdel Majid A. Adam*[1], *Hosam A. Saad*[1,3], *Ahmed M. Naglah*[4,5],
Mohamed A. Al-Omar[4]

[1] Department of Chemistry, Faculty of Science, Taif University, Al-Haweiah, P.O. Box 888, Zip Code 21974, Taif, Saudi Arabia
[2] Department of Chemistry, Faculty of Science, Port Said University, Port Said, Egypt
[3] Department of Chemistry, Faculty of Science, Zagazig University, Zagazig, Egypt
[4] Department of Pharmaceutical Chemistry, Drug Exploration & Development Chair, College of Pharmacy, King Saud University, Riyadh 11451, Saudi Arabia
[5] Peptide Chemistry Department, Chemical Industries Research Division, National Research Centre, 12622-Dokki, Cairo, Egypt
[*] E-mail: msrefat@yahoo.com

Received: 2 May 2015 / *Accepted:* 29 May 2015 / *Published:* 24 June 2015

A combined solution and solid state study was performed to describe the complexation chemistry of iodine with three highly fluorescent bis-1,8-naphthalimide dyes. The spectroscopic properties, photostability characteristics and the mechanism of interaction were investigated and discussed. The formed complexes were characterized stoichiometrically and structurally using ultraviolet-visible, mid- and far-infrared spectral techniques, as well as CHN elemental analyses. A remarkable change in the UV-Vis spectra was observed when the iodine acceptor was complexed with a 1:2 stoichiometry. Far-IR measurements confirmed the formation of triiodide (I_3^-). The formation constant, molar extinction coefficient and other spectroscopic data were also determined and discussed. It has been found that the complexation with iodine increases the photostability of the reported dyes. Interestingly, a strong linear correlation (r = 0.991) between half-life of photostability and dissociation energy in solution is clearly evidenced for the first time.

Keywords: 1,8-naphthalimide dyes, Charge-transfer complex, Iodine σ-acceptor, UV properties, Photostability properties.

1. INTRODUCTION

The study of the charge-transfer (CT) interaction of iodine as a σ-electron acceptor with various types of organic compounds, in general, is of importance and significant interest. The CT interactions between iodine and several types of electron donors such as aromatic hydrocarbons, polycyclic amines, aromatic/aliphatic amines, and mixed oxygen/nitrogen cyclic bases have been studied and categorized. Some of these systems show interesting physical properties, such as electrical conductivity. Additionally, some iodine complexes have been utilized in the pharmaceutical analysis of drugs in their pure form [1-10]. Fluorescent 1,8-naphthalimide dyes have a bright color and possess relatively high electron affinity and excellent transport properties [11]. They may be considered as important building blocks owing to their good chemical stability, large Stokes shift, and high fluorescent quantum yield [12]. These dyes have found applications in solar energy collectors, brightening of polymers, laser active media, organic light-emitting diodes, photosensitive biologically active units, fluorescent markers in biology, fluorescent sensors and in medicine as antitumors [13-17]. Fluorescent 1,8-naphthalimide dyes are a well-known, important class of electron donors. The studies of their CT interaction with iodine stem from their possible role in semiconductor applications. Thus, the mechanism of interaction of iodine with these dyes, in general, is a research topic of significant interest. Based on the interesting results obtained for the complexation properties of dyes with acceptors, in this research, as a continuation of our work in this field [18-23], the interactions of three highly fluorescent bis-1,8-naphthalimide dyes, namely, bis(*N*-ethyl-1,8-naphthalimide)amine (L1), bis(4-chloro-*N*-ethyl-1,8-naphthalimide) amine (L2) and bis(4-nitro-*N*-ethyl-1,8-naphthalimide)amine (L3), with iodine were investigated. Firstly, the fluorescent bis-1,8-naphthalimide dyes were synthesized. Then, their CT complexes with iodine were obtained and spectroscopically characterized both in solution and in the solid state. The formation constant (K_{CT}), molar extinction coefficient (ε_{CT}) and other spectroscopic data were calculated using Benesi–Hildebrand methods. Additionally, the photostability properties of these complexes as well as those of the free dyes were determined in chloroform at room temperature.

2. METHODOLOGY

2.1 Chemicals and spectral measurements

All of the chemicals used throughout this study were reagent grade, and all solutions were freshly prepared daily. The synthesized fluorescent dyes presented in Scheme 1, namely, bis(*N*-ethyl-1,8-naphthalimide)amine (L1), bis(4-chloro-*N*-ethyl-1,8-naphthalimide)amine (L2) and bis(4-nitro-*N*-ethyl-1,8-naphthalimide)amine (L3), were prepared according to literature methods [24]. The electron acceptor iodine (minimum assay 99.9%) and other spectroscopic grade solvents were purchased from Sigma-Aldrich and Merck Chemical Companies and were used without modification. Elemental analyses for the C, H and N contents of the solid compounds were carried out on a Perkin−Elmer CHN 2400 (USA). All of the electronic absorption spectral measurements were recorded in chloroform over a wavelength range of 200–800 nm using a Perkin–Elmer Lambda 25 UV/Vis double-beam spectrophotometer. The instrument was fitted with a quartz cell with a path length of 1.0 cm. IR spectra of the solid CT complexes (as KBR discs) were acquired at room temperature using a Shimadzu FT-IR spectrophotometer instrument (Japan) in the range of 4000–400 cm^{-1} for 30 scans at a 2 cm^{-1} resolution. Far-IR spectra for the solid CT complexes (as Nujol mulls dispersed on polyethylene windows) were recorded using a Mattson infinity series FT-IR TM high resolution vacuum spectrophotometer in the range of 300–50 cm^{-1}.

2.2 Reaction chemistry

To obtain the CT complexes, a chloroform solution of L1, L2 or L3 (1 mmol) was stirred with a chloroform solution of iodine (1 mmol) for *ca*. 30 min on a magnetic stirrer at room temperature. A change in color developed, and the volume of the solution was reduced to one-half by evaporation on a water bath, resulting in the precipitation of the solid CT complexes. The formed complexes were isolated as orange, bulbous (oniony), and lemon yellow color powdered material for $L1{-}I_2$, $L2{-}I_2$, and $L3{-}I_2$, respectively. The solid products were filtered off and washed twice thoroughly with the minimum given solvent to obtain the pure products. The products were then collected and dried *in vacuo* for 48 h. These complexes were characterized by spectroscopy (IR and UV-Vis) and elemental analysis.

2.3 Stoichiometric procedure

To determine the stoichiometry of the L1−iodine, L2−iodine and L3−iodine systems, various molar ratios were examined by spectrophotometric titration measurements. These titrations monitored the detectable CT bands during the reactions of L1, L2 or L3 with I_2 [25]. Briefly, 0.25, 0.50, 0.75, 1.00, 1.50, 2.0, 2.50, 3.00, 3.50 or 4.00 mL of a standard solution (5.0×10^{-4} M) of the appropriate acceptor in chloroform was added to 1.00 mL of the donor at 5.0×10^{-4} M, dissolved in the same solvent. The final volume of the mixture was 5 mL. The concentration of the donor (C_d) was maintained at 5.0×10^{-4} M, whereas the concentration of the acceptor (C_a) varied from 0.25×10^{-4} M to 4.00×10^{-4} M to produce solutions with a (donor: acceptor) molar ratio that varied from 4:1 to 1:4. The absorbance of each complex was plotted against the volume of the added acceptor [25].

2.4 Photostability measurements

The photostabilities of the dyes and their CT complexes doped in poly (methylmethacrylate) (PMMA) were determined by measuring the change in the absorption spectra at different times during irradiation [26]. The PMMA grains and the dye or complex were dissolved in chloroform and mixed using a magnetic stirrer. The homogeneous mixture was poured into a glass Petri dish container and allowed to dry. A solar simulator Xenon arc lamp (250 W), which had the same spectrum as the sun, was used to irradiate the samples for different periods of time (0, 3, 6, 9 and 12 h). The degradation of the samples was studied by analyzing the UV-Vis absorption spectra. The photostability was calculated by dividing the absorbance after light exposure by that before exposure [26].

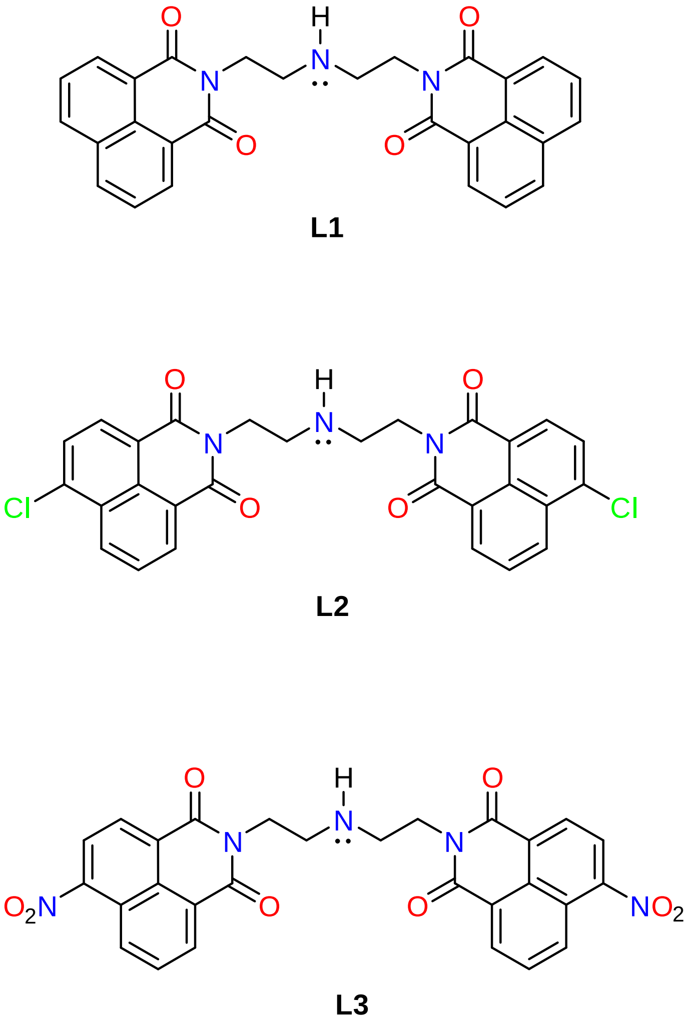

Scheme 1. Chemical structures of the synthesized L1, L2 and L3 fluorescence dyes

2.5 Calculations in solution

In the solution state, the spectroscopic data of the formed CT complexes were calculated as summarized below. The formation constant (K) and the molar extinction coefficient (ε) were determined spectrophotometrically using the 1:2 modified Benesi–Hildebrand equation (Eq. 1) [27, 28]. C_a and C_d are the initial concentrations of the acceptor and donor, respectively, and A is the absorbance of the CT band. By plotting the $(C_a)^2C_d/A$ values for the 1:2 CT complex as a function of the corresponding $C_a\ (4C_d + C_a)$ values, a straight line is obtained with a slope of $1/\varepsilon$ and an intercept at $1/K\varepsilon$. The energy values (E_{CT}) of the $n\rightarrow\pi^*$ and $\pi\rightarrow\pi^*$ interactions between the donor and the acceptor was calculated using the equation derived by Briegleb (Eq. 2) [29], where λ_{CT} is the wavelength of the complexation band. The oscillator strength (f) is a dimensionless quantity used to express the transition probability of the band. From the absorption spectra, f can be obtained using an approximate formula (Eq. 3) [30]. $\int \varepsilon_{CT}\, d\nu$ is the area under the curve of the extinction coefficient of the absorption band in question plotted as a function of the frequency. To a first approximation, f can be calculated using Eq. 4. ε_{CT} is the maximum extinction coefficient of the CT band, and $\nu_{½}$ is the full width at half maximum in cm^{-1}. The transition dipole moments (μ) are calculated using Eq. 5 [31]. The transition dipole moment (μ) can be employed to determine if a particular transition is allowed. The transition from a bonding π orbital to an antibonding π^* orbital is allowed because the integral that defines the transition dipole moment is nonzero. The ionization potential (I_P) of the highest filled molecular orbital of the donor was estimated from the CT energies of its complexes with the acceptor making use of the empirical equation reported by Aloisi and Pignataro (Eq. 6) [32]. The values of the standard free energy change ($\Delta G°$) were calculated from the formation constants using Eq. 7 [33]. $\Delta G°$ is the standard free energy change of the complexes (kJ mol^{-1}), R is the gas constant (8.314 J mol^{-1} K^{-1}), T is the absolute temperature in Kelvin, and K is the formation constant of the complex (L mol^{-1}) at room temperature. The dissociation energy (W) was calculated from the CT energy, E_{CT}, the ionization potential of the donor, I_P, and the electron affinity, E_A, of the acceptor using the empirical relation given in Eq. 8 [34]. The rate constants (k) of the photodegradation of the compounds were estimated using Eq. 9 [35, 36], where A_o and A are the absorbances before and after irradiation for time t.

$$(C_a)^2 C_d/A = 1/K\varepsilon + 1/\varepsilon\, C_a\,(4C_d + C_a) \qquad (1)$$

$$E_{CT} = (h\nu_{CT}) = 1243.667/\lambda_{CT}\ (\text{nm}) \qquad (2)$$

$$f = 4.319\times10^{-9} \int \varepsilon_{CT}\, d\nu \qquad (3)$$

$$f = 4.319\times10^{-9}\ \varepsilon_{CT}\ \nu_{½} \qquad (4)$$

$$\mu\ (\text{Debye}) = 0.0958\ [\varepsilon_{CT}\nu_{½}/\nu_{max}]^{½} \qquad (5)$$

$$I_P\ (\text{eV}) = 2.90 + 1.89\times10^{-4}\ \nu_{iodine}\ (cm^{-1}) \qquad (6)$$

$$\Delta G° = -2.303RT \log K_{CT} \qquad (7)$$

$$E_{CT} = I_P - E_A - W \qquad (8)$$

$$k = (2.303/t) \log A_0/A \qquad (9)$$

3. RESULTS AND DISCUSSION

3.1 Solution analyses

3.1.1 UV–Visible spectroscopy

Figure 1 displays the electronic absorption spectra of the donors (5.0×10^{-4} M) and iodine acceptor (5.0×10^{-4}), along with those of the prepared CT complexes. This figure indicates a remarkable change in the UV-Vis spectrum of the donor upon the addition of iodine to the solution. The spectra of the obtained complexes were characterized by two strong absorption bands at 245 and 340–355 nm. The donors display a strong broad band at 300 nm, while iodine displays no measurable absorption band at that wavelength. Interestingly, on mixing the solutions of the donors and iodine, this characteristic band red-shift, increases strongly in intensity, becomes more broad and is centered at 340, 355 and 340 nm for the L1–I_2, L2–I_2 and L3–I_2 complexes, respectively. These new strong broadening bands at longer wavelengths are presumably due to the dye–iodine interactions and are indicative of the formation of a CT complex.

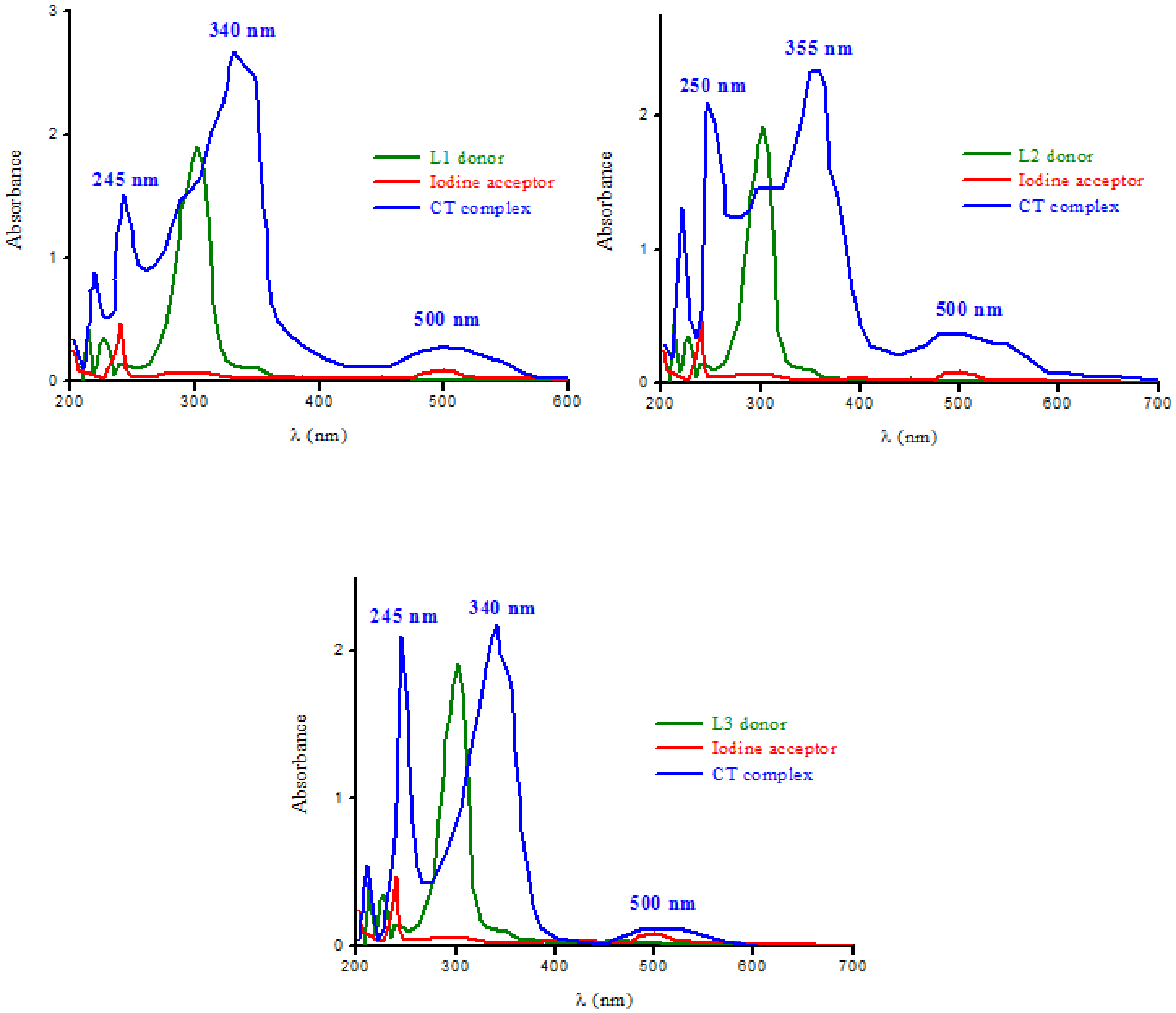

Figure 1. Electronic spectra for L1–I_2, L2–I_2 and L3–I_2 systems in chloroform solvent at 298 K.

3.1.2 Stoichiometry of the interaction

The stoichiometry of the formed CT complexes between the donors and the iodine acceptor was determined by applying a varying molar ratio spectrophotometric titration method. The electronic spectra of the dye–iodine systems were recorded with varying concentrations of iodine and a constant dye concentration. The compositions of the complexes were determined graphically by plotting the absorbance as a function of the volume of acceptor (in mL). Representative spectrophotometric titration plots based on the characterized absorption bands are shown in Figure 2. The results show that the largest interaction between each donor and iodine acceptor occurred at a dye:iodine ratio of 1:2. The stoichiometry of the L1–I_2, L2–I_2 and L3–I_2 systems were further confirmed by the elemental analyses of the formed solid complexes.

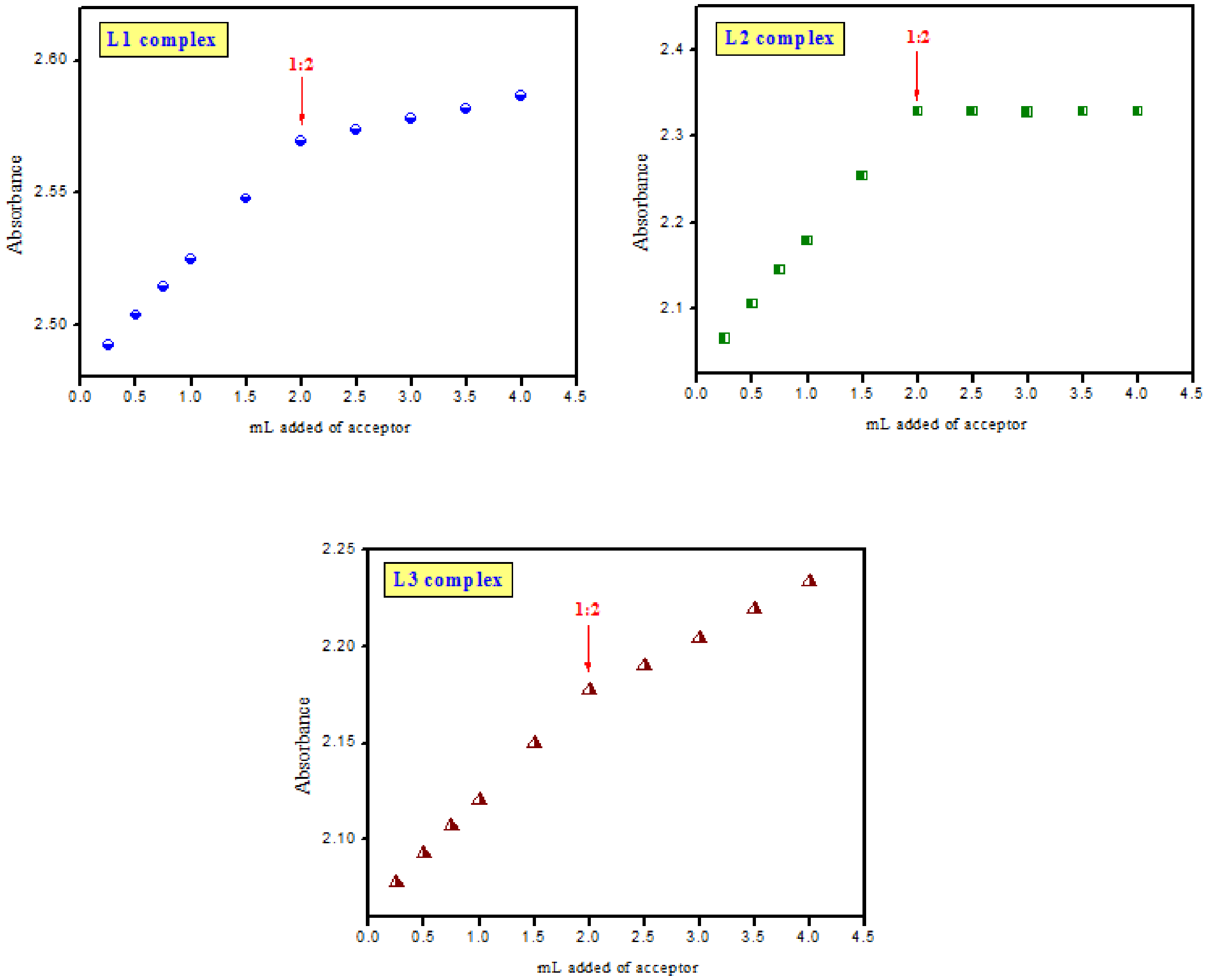

Figure 2. Spectrophotometric titration curves for L1–I_2, L2–I_2 and L3–I_2 systems in chloroform solvent at 298 K.

3.1.3 Spectroscopic data

The values of C_d, C_a, $C_a\,(4C_d + C_a)$ and $(C_a)^2C_d/A$ for the complexes are listed in Table 1. The values of $(C_a)^2C_d/A$ are plotted against the corresponding $C_a\,(4C_d + C_a)$ values for each donor with each acceptor.

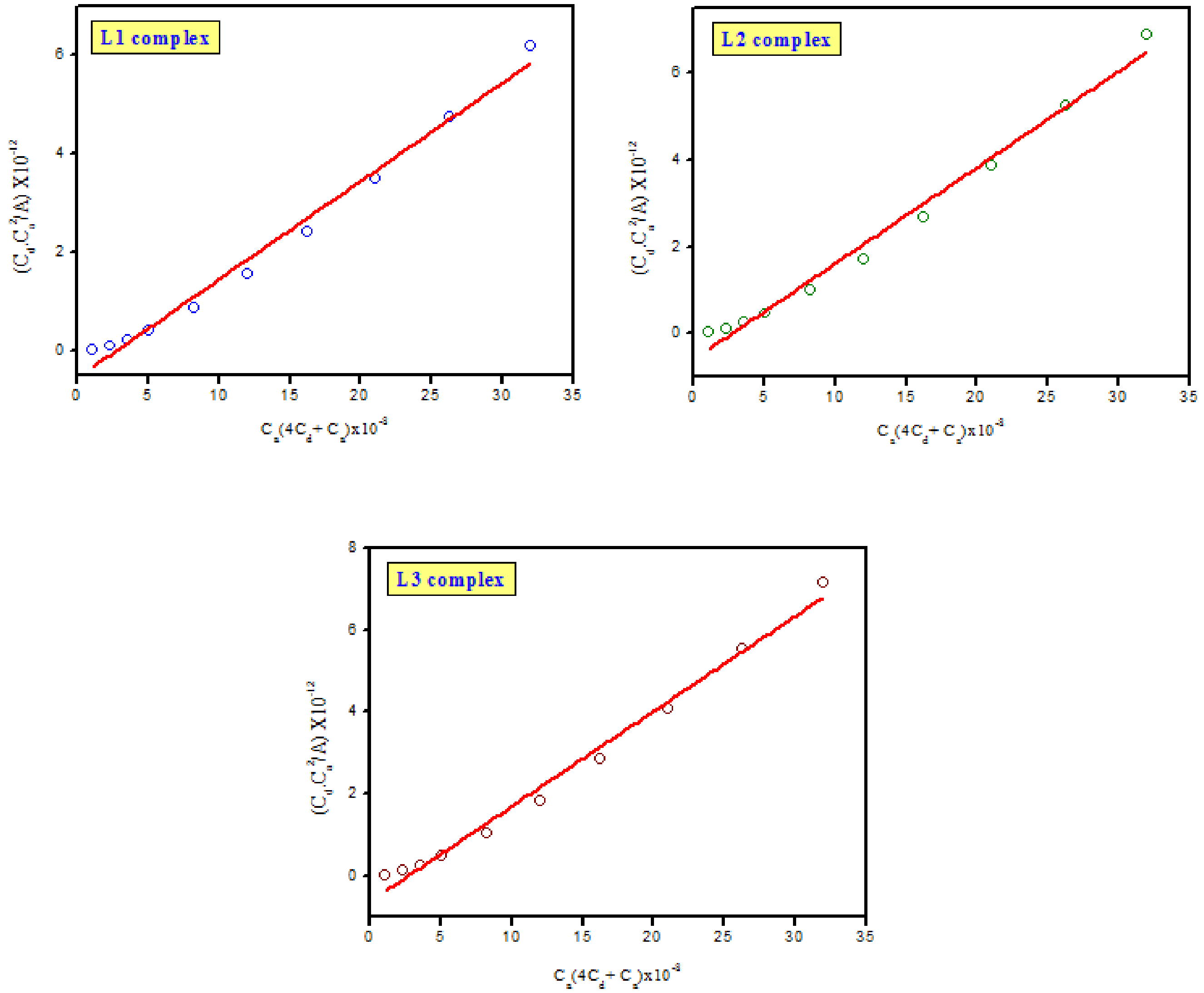

Figure 3. The 1:2 Benesi-Hildebrand plots for L1–I_2, L2–I_2 and L3–I_2 systems.

Table 1. The values of C_d, C_a, C_a $(4C_d + C_a)$ and $(C_a)^2C_d/A$, for the dye–iodine CT complexes.

Ratio (A:D)	C_d ($\times10^{-4}$)	C_a ($\times10^{-4}$)	C_a $(4C_d + C_a)$ ($\times10^{-6}$)	$(C_a)^2C_d$ ($\times10^{-12}$)	L1–I_2 complex		L2–I_2 complex		L3–I_2 complex	
					Abs. 340 nm	$(C_a)^2C_d/A$ ($\times10^{-12}$)	Abs. 355 nm	$(C_a)^2C_d/A$ ($\times10^{-12}$)	Abs. 340 nm	$(C_a)^2C_d/A$ ($\times10^{-12}$)
0.25	1.00	0.25	1.0625	0.0625	2.4920	0.0251	2.0659	0.0303	2.0777	0.0301
0.50	1.00	0.50	2.25	0.25	2.5034	0.0999	2.1058	0.1187	2.0930	0.1194
0.75	1.00	0.75	3.563	0.5625	2.5140	0.2237	2.1445	0.2623	2.1076	0.2669
1.00	1.00	1.00	5	1.00	2.5244	0.3961	2.1788	0.4590	2.1205	0.4716
1.50	1.00	1.50	8.25	2.25	2.5476	0.8832	2.2532	0.9986	2.1495	1.0468
2.00	1.00	2.00	12	4.00	2.5695	1.5567	2.3280	1.7182	2.1778	1.8367
2.50	1.00	2.50	16.25	6.25	2.5737	2.4284	2.3276	2.6852	2.1899	2.8540
3.00	1.00	3.00	21	9.00	2.5778	3.4913	2.3273	3.8671	2.2045	4.0826
3.50	1.00	3.50	26.25	12.25	2.5816	4.7451	2.3280	5.2620	2.2189	5.5208
4.00	1.00	4.00	32	16.00	2.5864	6.1862	2.3279	6.8731	2.2332	7.1646

Table 2. Spectral properties of the dye–iodine CT complexes in chloroform at 298 K.

Property	Complexes		
	L1–I_2	L2–I_2	L3–I_2
λ_{max} (nm)	340	355	340
Formation constant; K (Lmol^{-1})	3673	3725	3760
Extinction coefficient; ε_{max} (Lmol^{-1}cm^{-1})	50110	45244	43187
Energy value; E_{CT} (eV)	3.66	3.50	3.65
Oscillator strength; f	0.433	0.326	0.266
Dipole moment; μ	5.592	4.957	4.388
Ionization potential; I_p (eV)	8.459	8.224	8.350
Free energy; ΔG° (kJ mol^{-1})	-43165	-43199	-43222
Dissociation energy; W (eV)	1.74	1.67	1.64

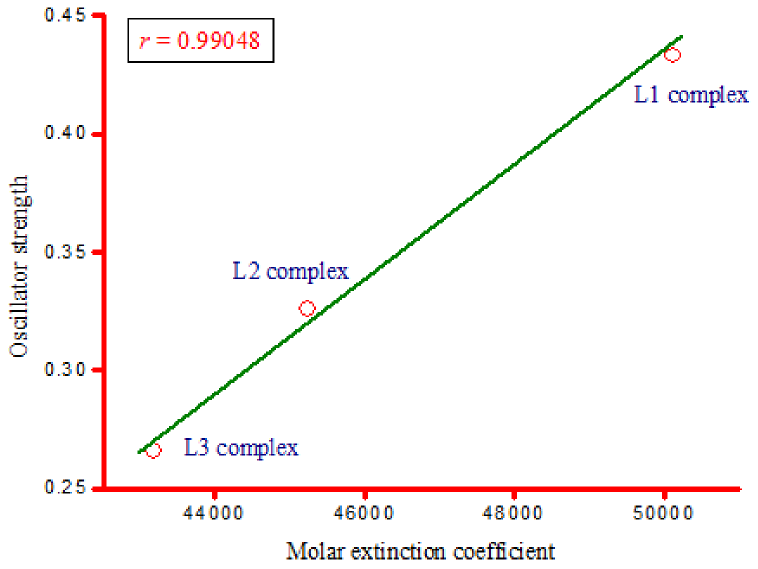

Figure 4. Linear correlation between molar extinction coefficient (ε) and oscillator strength (f) of the dye–iodine CT complexes.

A straight line was obtained with a slope of $1/\varepsilon$, and an intercept of $1/K\varepsilon$. Representative Benesi–Hildebrand plots are shown in Figure 3, and the values of both K and ε are thus determined and are given in Table 2 along with the other spectroscopic data (f, μ, E_{CT}, $\Delta G°$, I_P and W) calculated as previously described.

The obtained data of these CT complexes led to the following observations:

i) The complexes exhibit higher K values. The high values of K suggest that the CT complexes are strongly bound and highly stable. The Benesi–Hildebrand plots further supports this conclusion [37].

ii) The stability of the complexes decreases in the following order: $L3–I_2 > L2–I_2 > L1–I_2$.

iii) The complexes exhibit higher ε values. The high value of ε agrees quite well with the existence of the triiodide ion [38-41]. The ε values of the CT complexes decrease for the different donors as follows: L1 > L2 > L3.

iv) The L1–iodine complex exhibits higher values of both f and μ, which indicates a strong interaction between dye and iodine acceptor with relatively high probabilities of CT transitions.

A liner relationship was obtained between the molar extinction coefficient (ε) and the oscillator strength (f) of the dye–iodine complexes (Figure 4). The correlation coefficient (r) for the straight line was found to be 0.99. This finding indicates that the value of f increases with the increase of ε.

v) All of the $\Delta G°$ values are negative. These negative values indicate that the interaction between the dyes and the iodine is spontaneous.

vi) The $\Delta G°$ values of the complexes in decreasing order for the different donors are as follows: L3 > L2 > L1.

vii) The calculated I_P values for the molecular orbitals participating in the CT interactions of the L1, L2 and L3 donors were 8.46, 8.22 and 8.35 eV, respectively.

viii) The calculated values of the dissociation energy (W) indicate that the obtained complexes are strong and stable and having high resonance stabilization energy [37, 42, 43].

3.1.4 Photostability results

All fluorescent dyes undergo photobleaching after prolonged exposure to sunlight. Because of the high E_{CT} and melting point of the donors, we decided to check their photostabilities and those of their CT complexes with iodine. The photochemical degradation of the investigated compounds occurs only in the presence of suitable optical radiation producing large local increases in temperature and thermal destruction of the dye molecules. Figure 5 shows the change in the absorption spectra during the irradiation period (0, 3, 6, 9 and 12 h); the k values and half-lifes ($t_{½}$) are listed in Table 3.

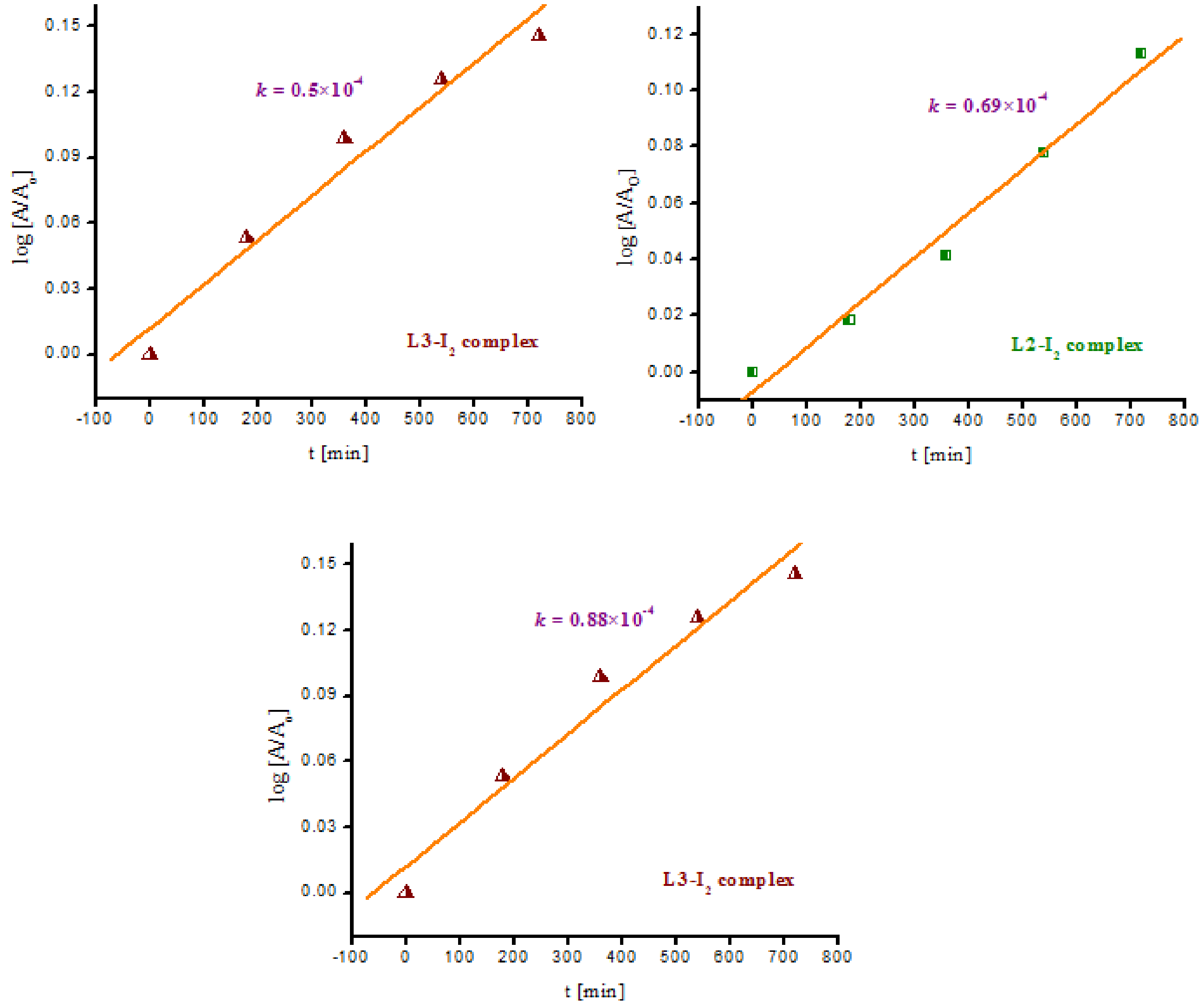

Figure 5. Photostability of L1–I_2, L2–I_2 and L3–I_2 complexes doped in PMMA before and after exposure to UV–Vis light.

Table 3. Rate constant (*k*) of photostability and half-lifes of the dye–iodine CT complexes.

Compound	Property	
	Rate constant; *k* (min^{-1})	Half–lifes; $t_{½}$ (min)
L1	0.93×10^{-4}	7487
L1–I_2 complex	0.50×10^{-4}	13899
L2–I_2 complex	0.69×10^{-4}	10067
L3–I_2 complex	0.88×10^{-4}	7904

L1–I_2 complex showed a $t_{½}$ of about 13900 min. that become approximately two fold higher in free L1 donor ($t_{½}$ = 7490 min.).

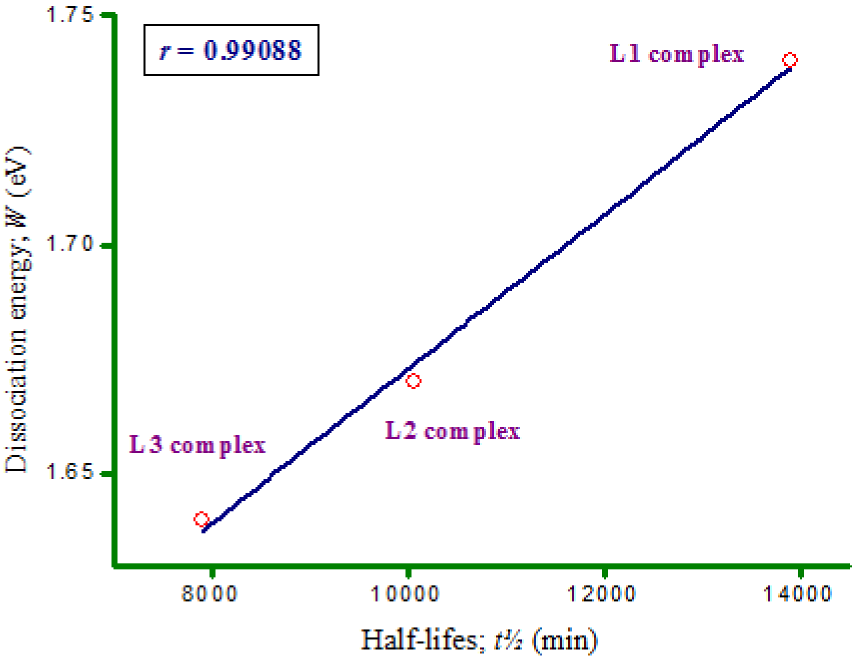

Figure 6. Linear correlation between half-lifes (*t*) and dissociation energy (*W*) of the dye–iodine CT complexes.

It is clear from the degradation data that the complexation with iodine acceptors improves and increases the photostability of the dye. This increased photostability is presumably due to the strong chelation between the donor and iodine acceptor. Figure 6 clearly shows that a strong linear correlation (r = 0.991) was obtained by plotting the half-lifes ($t_{½}$) of photodegradation as a function of the dissociation energy (*W*) of the dye–iodine CT complexes. This finding indicates that the photostability of the CT complexes increased with the increase of their dissociation energy values.

3.2 Solid analyses

3.2.1 Elemental analysis results

The synthesized solid complexes were analyzed in terms of their carbon, hydrogen, and nitrogen content in order to determine the stoichiometry of the complex formation. The elemental analysis data were in satisfactory agreement with the calculated values. The results of the elemental analyses of the formed CT complexes are as follows. (L1–I_2): $C_{28}H_{21}N_3O_4I_3$; Mol. wt. = 844.2; Calc.: %C, 39.84; %H, 2.51; %N, 4.98, Found: %C, 39.80; %H, 2.49; %N, 4.96. (L2–I_2): $C_{28}H_{19}N_3O_4Cl_2I_3$; Mol. wt. = 913.09; Calc.: %C, 36.83; %H, 2.1; %N, 4.6, Found: %C, 36.86; %H, 2.13; %N, 4.57. (L3–I_2): $C_{28}H_{19}N_5O_8I_3$; Mol. wt. = 934.19; Calc.: %C, 36.0; %H, 2.05; %N, 7.5, Found: %C, 35.96; %H, 2.01; %N, 7.54. The stoichiometry of the interaction between the donors and the iodine acceptor was found to be 1:2. The results of the elemental analyses confirmed the stoichiometry determined by the spectrophotometric titrations.

3.2.2 Mid-infrared spectral analysis

The characteristic mid-IR peak assignments of the free donors and of their corresponding solid CT products are reported in Table 4.

Table 4. Mid–IR wavenumbers (cm^{-1}) and tentative band assignments for the free donors and their CT complexes.

Donors			CT complexes			Assignments
L1	L2	L3	L1–I_2	L2–I_2	L3–I_2	
3337	3425	3330	3240	3263	3449	ν(N–H)
3065	3077	3067	3063	3071	3068	ν(C–H); aromatic
2960	2959	2957	2916	2925	2926	ν(C–H); aliphatic
2837	2832	2829	2855		2856	
1697	1706	1702	1696	1704	1730	ν_{as}(C=O)
1661	1664	1661	1650	1660	1661	ν_{s}(C=O)
1588	1586	1588	1586	1584	1590	δ(N–H)
1342	1342	1345	1343	1344	1349	ν(C–N)
778	786	780	780	786	782	Aromatic ring deformation.

The mid-IR spectra of the free donors L1, L2 and L3 show the following distinguished absorption bands: *(i)* a broad band of ν(N–H) at 3337, 3425 and 3330 cm^{-1} for L1, L2 and L3, respectively; *(ii)* bands at 3077–3065 cm^{-1} assigned to ν(C–H) aromatic vibrations; *(iii)* a broad band at 2960–2837, 2959–2832 and 2957–2829 cm^{-1} in L1, L2 and L3, respectively, assigned to the vibration of –CH_2– groups; *(iv)* L1, L2 and L3 show intensive absorption bands at 1661–1697, 1664–1706 and 1661–1702 cm^{-1}, respectively, which are characteristic of the symmetric ν_s and asymmetric ν_{as} carbonyl group vibrations; *(v)* bending vibrations of δ(N–H) appearing at ~ 1587 cm^{-1}; *(v)* stretching C–N vibration at approximately 1342 cm^{-1}; *(vi)* bands at 1624–1623 and 1507–1527 cm^{-1}, assigned to ν(C=C) vibrations. These are characteristic of the aromatic system in the naphthalene ring of the naphthalimide structure; and *(vii)* bands at 778–786 cm^{-1}, characteristic of the deformation vibrations of aromatic rings. When iodine was complexed with the dyes, the characteristic ν(C–N) and ν(N–H) vibration peaks of the free donors were shifted and exhibited decreased intensities. The observed shift in both the ν(C–N) and ν(N–H) bands upon complexation clearly indicated that the –NH moiety of the donors participated in the CT bonding with iodine. The vibrational absorption band of δ(N–H) was shifted to higher frequencies in the L1 and L3 complexes and to lower frequencies in the L2 complex. Furthermore, the carbonyl stretching vibration bands, ν(C=O), slightly shifted with respect to those of the free donors; this is most likely due to intermolecular CT interactions. Such shifts suggest electron transfer from the N atom of the donors to the iodine molecule to form the corresponding triiodide complex.

3.2.3 Far-infrared spectral analysis

Table 5. Far–IR wavenumbers (cm^{-1}) and tentative band assignments for the L1–I_2 and L2–I_2 CT complexes.

CT complexes		Assignments
L1–I_2	L2–I_2	
254	251	Free I_2
161	142	ν_{as}(I–I)
123	112	ν_s(I–I)
93	75	$\delta(I_3^-)$

Far-infrared spectroscopy can provide valuable information on the nature and structural features of polyiodide anions. The characteristic far-IR peak assignments of the L1–I_2 and L2–I_2 CT complexes are reported in Table 5. The spectra of these two complexes contained the characteristic bands for triiodide (I_3^-) at 161–142, 123–112 and 93–75 cm^{-1}, corresponding to ν_{as}(I–I), ν_s(I–I) and $\delta(I_3^-)$, respectively. The observed sharp peaks at 254–251 cm^{-1} could be due to the presence of unreacted free iodine. Maki and Forneris [44] assigned the lines of I_3^- at 112 and 161 cm^{-1} to the symmetric and antisymmetric stretching vibrations, respectively. The literature data [45–49] generally indicate that the linear and symmetric I_3^- species is far-IR active, with a symmetric stretch (ν_s) in the region of 100–120 cm^{-1} and an antisymmetric stretch (ν_{as}) in the 130–155 cm^{-1} range. The bending (δ) deformation becomes active for the antisymmetric I_3^- ion, in the region near 80 cm^{-1}. The I_3^- ion may be linear (D_h) or nonlinear (C_{2v}). Group theoretical analysis indicates that the I_3^- has a C_{2v} symmetry and displays three vibrations, including ν_{as}(I–I), A_1, ν_s(I–I), B_2, and δ, (I_3^-), A_1. All of these vibrations are IR active, which agrees well with the observation of the three far-IR bands for the $[L1–I]^+I_3^-$ and $[L2–I]^+I_3^-$ complexes. The observed far-IR spectra confirmed the formation of the antisymmetric triiodide ion.

3.2.4 Reaction mechanism

According to the above discussion, the prepared CT complexes could be represented as $[L1–I]^+I_3^-$, $[L2–I]^+I_3^-$ and $[L3–I]^+I_3^-$. A general mechanism is proposed for the formation of the $[Dye–I]^+I_3^-$ complex as follows: the dye initially forms an outer complex with iodine in a fast step, followed by its transformation into an inner complex, followed by a fast reaction of the resulting inner complex with another mole of iodine to form a triiodide (I_3^-) ion, as depicted below.

$Dye + I_2 \leftrightarrows Dye–I_2$ (outer complex) Fast
$Dye–I_2 \leftrightarrows [Dye–I]^+I^-$ (inner complex) Slow
$[Dye–I]^+I^- + I_2 \leftrightarrows [Dye–I]^+I_3^-$ (triiodide complex) Fast

The formation of the $[Dye–I]^+I^-$ reaction intermediate is analogous to that of the well-known species $[base–I]^+I^-$ formed in the reaction of iodine with many donors. The literature data indicate that the band representing the bending deformation of the antisymmetric triiodide ion, $\delta(I_3^-)$, appears in the region near 80 cm^{-1}. In the far-IR spectra of the L1–I_2 and L2–I_2 complexes, this line was split into two peaks at 93 and 75 cm^{-1}. This finding may be attributed to an electron transfer from the N atom of the donor to the middle iodine atom in the triiodide ion, as opposed to one of the terminal iodine atoms. Thus, it can be concluded that the reaction of iodine with the investigated florescent dyes results in triiodide complexes, $[\text{Dye-I}]^{+}I_3^{-}$, where the I_3^{-} ion chelates through the middle iodine atom. Accordingly, the proposed structures of the formed CT complexes are represented in Scheme 2.

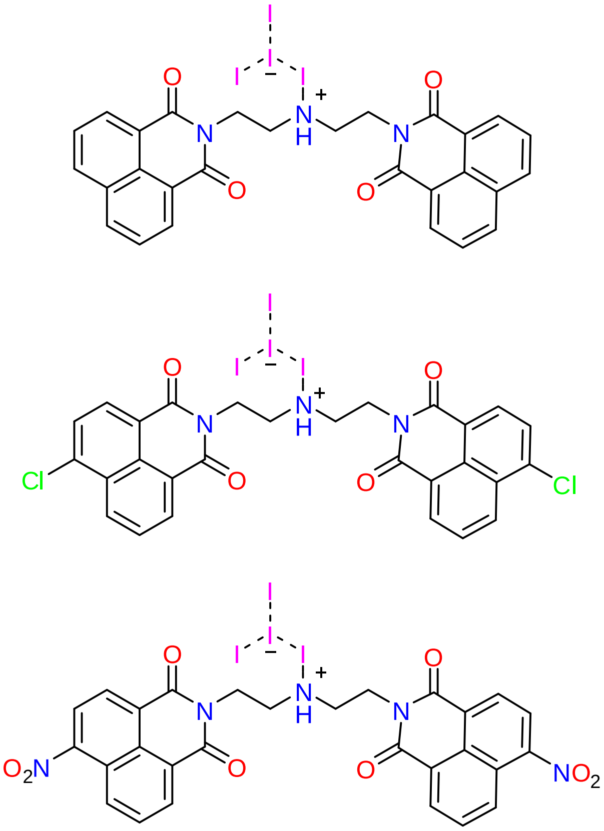

Scheme 2. Proposed structural formula of the L1–I_2, L2–I_2, L3–I_2 complexes.

4. CONCLUSIONS

In this work, we successfully synthesized three dye–iodine complexes. Significant changes in the Ultraviolet-Visible spectra were observed. Binding ratio of dye:iodine was determined to be 1:2 according to the elemental analyses and spectrophotometric measurements. The three dye–iodine systems were characterized by the formation of the antisymmetric triiodide ion, the presence of which was confirmed in the far-IR spectra. The interaction of dye with iodine was proceeded through three steps, namely, outer complex formation, conversion it to inner complex and tiriodie formation. The photostability of the obtained complexes was also investigated under UV-Vis light exposure. The results show a high stability of the complexes compared with the free donors. Moreover, the photostability of the CT complexes in solution increased with increase of their dissociation energy values.

ACKNOWLEDGEMENT
The authors would like to extend their sincere appreciation to the Deanship of Scientific Research at King Saud University for its funding of this work through the Research Group no: RG-1436-015.

References

1. K. Ganesh and K.P. Elango, *Spectrochim. Acta A*, 93 (2012) 185.
2. M.S. Refat, S.A. El-Korashy, I.M. El-Deen and S.M. El-Sayed, *J. Mol. Struct.,* 980 (2010) 124.
3. A. Mostafa and H.S. Bazzi, *J. Mol. Struct.*, 983 (2010) 153.
4. M. Pandeeswaran and K.P. Elango, *Spectrochim. Acta A*, 72 (2009) 789.
5. U.M. Rabie, M.H.M. Abou-El-Wafa and H. Nassar, *Spectrochim. Acta A,* 78 (2011) 512.
6. S.Y. AlQaradawi, H.S. Bazzi, Adel Mostafa and E. Nour, *J. Mol. Struct.*, 998 (2011) 126.
7. M.S. Refat, *J. Mol. Struct.*, 985 (2011) 380.
8. A.A. Gouda, Talanta, 80 (2009) 151.
9. L. Shahada, A. Mostafa, E. Nour and H.S. Bazzi, *J. Mol. Struct.*, 933 (2009) 1.
10. M.S. Refat, W.F. El-Hawary and M.A.A. Moussa, *Spectrochim. Acta A*, 78 (2011) 1356.
11. I. Grabchev and T.Z. Philipova, *Dyes Pigments*, 27 (1995) 321.
12. Y. Li, Y. Xu, X. Qian and B. Qu, *Tetrahedron Lett.*, 45 (2004) 1247.
13. D. Staneva, P. Bosch, A. M. Asiri, L. A. Taib and I. Grabchev, *Dyes Pigments*, 105 (2014) 114.
14. I. Grabchev, D. Staneva and R. Betcheva, *Curr. Med. Chem.*, 29 (2012) 4976.
15. Z. Li, Y. Zhou, K. Yin, Z. Yu, Y. Li and J. Ren, *Dyes Pigments*, 105 (2014) 7.
16. F. Sun and R. Jin, *J. Luminescence*, 149 (2014) 125.
17. E. Tamanini, A. Katewa, L. Sedger, M. Todd and M. Watkinson, *Inorg. Chem.*, 48 (2009) 319.
18. M.S. Refat, I. Grabchev, J.-M. Chovelon and G. Ivanova, *Spectrochim. Acta A*, 64 (2006) 435.
19. M.S. Refat, H.M.A. Killa, I. Grabchev and M.Y. El-Sayed, *Spectrochim. Acta A*, 68 (2007) 123.
20. M.S. Refat, A.H. El-Didamony, Kh.M. Abou El-Nour, I. Grabchev and L. El-Zayat, *Bulg. Chem. Commun*, 42 (4) (2010) 279.
21. M.S. Refat, S.M. Aqeel and I. Grabchev, *Can. J. Anal. Sci. Spectrosc.*, 49 (2004) 258.
22. M.S. Refat, H.A. Ahmed, I. Grabchev and L.A. El-Zayat, *Spectrochim. Acta A*, 70 (2008) 907.
23. M.S. Refat, S.M. Teleb and I. Grabchev, *Spectrochim. Acta A*, 61 (2005) 205.
24. I. Grabchev, C. Petkov and V. Bojinov, *Dyes Pigments*, 48 (2001) 239.
25. M.S. Refat, A.A. Gobouri, A.M.A. Adam and H.A. Saad, *Phys. Chem. Liqs.*, 52 (5) (2014) 680.
26. M.S. Refat, *J. Them. Anal. Calorim.*, 102 (2010) 1095.
27. H.A. Benesi and J.H. Hildebrand, *J. Am. Chem. Soc.*, 71 (1949) 2703.
28. R. Abu-Eittah and F. Al-Sugeir, *Can. J. Chem.*, 54 (1976) 3705.
29. G. Briegleb, *Z. Angew. Chem.*, 76 (1964) 326.
30. H. Tsubomura and R.P. Lang, *J. Am. Chem. Soc.*, 83 (1961) 2085.
31. R. Rathore, S.V. Lindeman and J.K. Kochi, *J. Am. Chem. Soc.*, 119 (1997) 9393.
32. G.G. Aloisi and Pignataro, *J. Chem. Soc. Faraday Trans.*, 69 (1973) 534.
33. A.N. Martin, J. Swarbrick and A. Cammarata, Physical Pharmacy, third edn., Lee and Febiger, Philadelphia, PA, 1969, p. 344.
34. I. Isenberg and S.L. Baird, *J. Am. Chem. Soc.*, 84 (1962) 3803.
35. I. Grabchev and V. Bojinov, *Polym. Degrad. Stab.*, 70 (2000) 147.
36. V.B. Bojinov and I. Grabchev, *Polym. Degrad. Stab.*, 74 (2001) 543.
37. K. Ganesh and K.P. Elango, *Spectrochim. Acta A*, 93 (2012) 185.

38. E-M. Nour, S.M. Teleb, M.A.F. Elmosallamy and M.S. Refat, *S. Afr. J. Chem.*, 56 (2003) 10.
39. W. Kiefer and H.J. Bernstein, *Chem. Phys. Lett.* 16 (1972) 5.
40. L. Andrews, E.S. Prochaska and A. Loewenschuss, *Inorg. Chem.*, 19 (1980) 463.
41. K. Kaya, N. Mikami, Y. Udagawa and M. Ito, *Chem. Phys. Lett.*, 16 (1972) 151.
42. M. Pandeeswaran and K.P. Elango, *Spectrochim. Acta A*, 72 (2009) 789.
43. R. Rathone, S.V. Lindeman and J.K. Kochi, *J. Am. Chem. Soc.*, 119 (1997) 9393.
44. A.G. Maki and R. Forneris, *Spectrochim. Acta A*, 23 (1967) 867.
45. E.M. Nour, L.H. Chen and J. Lanne, *J. Phys. Chem.*, 90 (1986) 2841.
46. E.M. Nour and L.A. Shahada, *Spectrochim. Acta A*, 45 (1989) 1033.
47. E.M. El-Neema, *Spectrochim. Acta A*, 60 (2004) 3181.
48. M. Pandeeswaran and K.P. Elango, *J. Sol. Chem.*, 38 (12) (2009) 1558.
49. K. Ganesh, C. Balraj and K.P. Elango, *Spectrochim. Acta A*, 79 (2001) 1621.

© 2015 The Authors. Published by ESG (www.electrochemsci.org). This article is an open access article distributed under the terms and conditions of the Creative Commons Attribution license (http://creativecommons.org/licenses/by/4.0/).